




# BAG3 induces fibroblasts to release key cytokines involved in pancreatic cell migration

Beatrice Dufrusine<sup>1,2</sup> | Verena Damiani<sup>1,2</sup> | Emily Capone<sup>1,2</sup> |  
 Damiana Pieragostino<sup>1,2</sup> | Enrico Dainese<sup>3</sup> | Margot De Marco<sup>4,5</sup> |  
 Francesca Reppucci<sup>4</sup> | Maria C. Turco<sup>4,5</sup>  | Alessandra Rosati<sup>1,4,5</sup>  |  
 Liberato Marzullo<sup>4,5</sup> | Gianluca Sala<sup>1,2</sup> | Michele Sallese<sup>1,2</sup>  |  
 Vincenzo De Laurenzi<sup>1,2</sup>

<sup>1</sup>Department of Innovative Technologies in Medicine and Dentistry, University of Chieti-Pescara, Chieti, Italy

<sup>2</sup>Center for Advanced Studies and Technology (CAST), University of Chieti-Pescara, Chieti, Italy

<sup>3</sup>Faculty of Bioscience and Technology for Food Agriculture and Environment, University of Teramo, Teramo, Italy

<sup>4</sup>Department of Medicine, Surgery and Dentistry Schola Medica Salernitana, University of Salerno, Baronissi, Italy

<sup>5</sup>R&D Division, BIOUNIVERSA s.r.l., Baronissi, Italy

## Correspondence

Michele Sallese and Vincenzo De Laurenzi, Department of Innovative Technologies in Medicine and Dentistry, Center for Advanced Studies and Technology, “G. d’Annunzio” University of Chieti-Pescara, 66100 Chieti, Italy.  
 Email: [michele.sallese@unich.it](mailto:michele.sallese@unich.it) and [del Laurenzi@unich.it](mailto:del Laurenzi@unich.it)

## Funding information

Associazione Italiana per la Ricerca sul Cancro, Grant/Award Number: IG-20043; POR CAMPANIA FESR 2014-2020 “SYSTEM INNOVATION FOR CANCER EARLY DIAGNOSIS SICED

## Abstract

Pancreatic ductal adenoma carcinoma (PDAC) is considered one of the deadliest solid cancers as it is usually diagnosed in advanced stages and has a poor response to treatment. The enormous effort made in the last 2 decades in the oncology field has not led to significant progress in improving early diagnosis or therapy for PDAC. The stroma of PDAC plays an active role in tumour initiation and progression and includes immune cells and stromal cells. We previously reported that Bcl2-associated athanogene (BAG3) secreted by PDAC cells activates tumour-associated macrophages to promote tumour growth. The disruption of this tumour–stroma axis by the anti-BAG3 H2L4 therapeutic antibody is sufficient to delay tumour growth and limit metastatic spreading in different PDAC preclinical models. In the present study, we examined the role of BAG3 to activate human fibroblasts (HF) in releasing cytokines capable of supporting tumour progression. Treatment of fibroblasts with recombinant BAG3 induced important changes in the organisation of the cytoskeleton of these cells and stimulated the production of interleukin-6, monocyte chemoattractant protein-1/C–C motif chemokine ligand 2, and hepatocyte growth factor. Specifically, we observed that BAG3 triggered a depolymerisation of microtubules at the periphery of the cell while they were conserved in the perinuclear area. Conversely, the vimentin-based intermediate filaments increased and spread to the edges of the cells. Finally, the conditioned medium (CM) collected from BAG3-treated HF promoted the survival, proliferation, and migration of the PDAC cells. Blocking of the PDAC-fibroblast axis by the H2L4 therapeutic anti-BAG3

antibody, resulted in inhibition of cytokine release and, consequently, the inhibition of the migratory phenotype conferred by the CM to PDAC cells.

#### KEYWORDS

BAG3, CCL2, cytokines, fibroblasts, HGF, pancreatic ductal adenoma carcinoma

## 1 | INTRODUCTION

With a 5-year overall survival (OS) rate ranging from 4% to 9% pancreatic ductal adenoma carcinoma (PDAC) is considered to be one of the deadliest solid cancers, accounting for 495 773 new cases and 466 003 deaths occurring in 2020.<sup>1</sup> Despite the enormous effort made in the last 2 decades in the oncology arena, no significant progress has been made in improving both early diagnosis and therapy for PDAC, leaving this malignancy as an incurable disease. Pancreatic cancer is usually diagnosed in advanced stages and has a poor response to treatments. Currently, radiation, combination cytotoxic chemotherapy, and molecular-targeting therapies are minimally effective for PDAC and radical surgery is the primary treatment. The PDAC resistance to therapies is mediated by its dense functional stroma, composed of extracellular matrix and characterised by the development of extensive fibrosis termed desmoplasia.<sup>2</sup> Furthermore, emerging therapies of PDAC with agents targeting specific proteins to interfere with stromal formation and function have shown good results in pre-clinical studies.<sup>3</sup> Nowadays, there are no tests or methods to choose the treatment protocols or predict response or prognosis. Hence, we need to improve our understanding of the complex biochemical cancer–stroma crosstalk in PDAC and to combine antistroma therapy with the conventional therapeutic approaches.

Large-scale omics studies have significantly contributed to the identification of several genetic and epigenetic alterations which drive molecular mechanisms involved in the initiation and progression of pancreatic cancer. However, the progress obtained in the knowledge of the PDAC genetic and epigenetic landscape has not yet translated into the development of novel therapeutics able to increase the survival of patients affected by this tumour. One of the possible explanations behind the difficulty to develop efficient drugs for PDAC therapy relies on the particular tissue structure of the tumour. Indeed, cancer cells represent only a minority of the tissue mass while the fibrotic represent the major component. Accordingly, it is now universally recognised that this dense fibrotic stroma plays an active role in determining tumour growth and metastatic spreading as well as resistance to

chemotherapeutics.<sup>4</sup> Indeed, fibrotic desmoplasia is recognised as one of the hallmarks of PDAC development. Different aspects characterise the transformation of the fibrotic component of pancreatic tumours: i) recruitment of specialised stroma cells such as fibroblasts and tumour-associated macrophages, and ii) deposition and remodelling of ECM (extracellular matrix) component, modulation of immunosurveillance (i.e., cells involved in antitumour immunity).<sup>5</sup> All these factors can determine in a concerted way the outcome of tumour growth and above all the response to therapies. It is, therefore, urgent to fully unveil intricate cancer–stroma interaction to develop novel targeted therapeutics.

In this scenario, our group has recently identified BAG3 as a PDAC secreted protein able to bind and activate macrophages to produce protumoral cytokines which sustain tumour growth.<sup>6</sup> The disruption of this tumour–stroma axis by the anti-BAG3 H2L4 therapeutic antibody has shown to be sufficient to delay tumour growth and limit metastatic spreading in different PDAC preclinical models.<sup>7</sup> Moreover, BAG3 inhibition obtained by antibody treatment increased anti-PD1 activity through the increase of CD8<sup>+</sup> infiltrate at the site of the tumour, therefore corroborating the hypothesis that BAG3 has a functional role in the interplay occurring between tumour and stroma PDAC cells.

In this study we analyzed the ability of BAG3 to activate fibroblasts in releasing cytokines capable of promoting proliferation and migration of PDAC cells.

## 2 | MATERIALS AND METHODS

### 2.1 | Preparation of recombinant BAG3

Recombinant baculovirus expressing BAG3 was constructed using the Gateway system (Invitrogen). Briefly, the Bag3 open reading frame was assembled by synthesis, cloned into pENTR\_3C\_Dual Vector, and sequence-verified (GeneArt Gene Synthesis Service; Invitrogen). Recombinant baculoviruses were prepared according to the manufacturer's instruction for BaculoDirect™ C-Term Transfection Kit (Invitrogen). Recombination was validated by polymerase chain reaction (PCR) using an internal gene-specific primer for BAG3 (5'-GCAGGTTTACGAACTGCAGCC-3') and a

specific primer for V5 epitope on baculovirus DNA (5'-ACCGAGGAGAGGGTTAGGGAT-3'). BAG3-containing baculoviral vector was transfected in insect Sf9 cells with Cellfectin reagent (Invitrogen) and recombinant baculovirus stock (P1) was recovered in the cell culture medium after 72 h. Viral stock P1 was amplified by infecting Sf9 cells for 72 h to prepare a high-titre viral stock. The titre of baculovirus stock was determined using BacPAK Baculovirus Rapid Titer Kit (Takara/Clontech). BAG3 was produced in Sf9 cells infected for 72 h with the recombinant baculoviruses at the multiplicity of infection of 8. Insect PopCulture® Reagent (Novagen) was used to extract protein from total insect cell culture (cell lysate and culture medium). The clarified extract was mixed with Ni-NTA His•Bind resin and shaken at 200 rpm on a rotary shaker at 4°C overnight. The lysate-Ni-NTA His•Bind mixture was loaded into a chromatography column, extensively washed with 300 mM NaCl, 50 mM sodium phosphate, 20 mM imidazole, pH 8, and the bound proteins eluted with the same buffer containing 250 mM of imidazole. Collected fractions were analysed on a 10% sodium dodecyl sulphate–polyacrylamide gel electrophoresis (SDS-PAGE). The fractions containing BAG3 were pooled, dialysed against 20 mM phosphate-buffered saline (PBS) pH 7.4, and concentrated by ultrafiltration on a Centricon (Merck Millipore) (cutoff 10 kDa). Protein concentration was measured with Bradford reagent (Bio-Rad), enzyme-linked immunosorbent assays (ELISA; Abcam), and Coomassie blue staining after SDS-PAGE with known concentrations of bovine serum albumin as quantification standard. The authenticity and the grade of BAG3 purification were analysed by Western blot and liquid chromatography (LC)-electrospray ionisation-quadrupole time-of-flight-mass spectrometry (MS/MS) according to the previously published protocol.<sup>8</sup>

## 2.2 | Western blotting analysis

Sf9 cells were lysed by radioimmunoprecipitation assay lysis buffer (Thermo Fisher Scientific, Inc.) supplemented with a protease inhibitor cocktail (Sigma-Aldrich). Cellular and supernatant protein amount was determined using the Bradford reagent (Bio-Rad). Ten micrograms of total protein were separated on 10% SDS-PAGE and transferred to the polyvinylidene fluoride membrane (Merck Millipore). The membranes were blocked in 5% skimmed milk in Tris-buffered saline buffer with 1% Tween-20 for 1 h at room temperature (RT), followed by incubation with primary antibodies overnight at 4°C. Subsequently, the membranes were incubated with horseradish peroxidase-conjugated secondary antibodies, detected by enhanced chemiluminescence solution (Pierce; Thermo Fisher Scientific, Inc.). The antibodies in this study included BAG3 (1:3000; Novusbio),

6His Tag (1:5000; Abcam), vimentin (1:1000; Cell Signaling Technology, Inc.), and glyceraldehyde-3-phosphate dehydrogenase (1:1000; Cell Signaling Technology, Inc.).

## 2.3 | Cell culture and treatments

Sf9 cells were obtained from Invitrogen and were grown in monolayer in Grace's Insect medium (Gibco; Thermo Fisher Scientific, Inc.) supplemented with 10% fetal bovine serum (FBS) (Gibco) at 27°C in a nonhumidified and nongas-regulated environment. For protein production, Sf9 cells were grown in suspension culture condition in Sf-900 III SFM (Gibco) medium with 2% FBS. The human monocytes were cultured in Roswell Park Memorial Institute-1640 medium supplemented with 10% FBS at 37°C in 5% CO<sub>2</sub>. The human fibroblast (HF) cell line was purchased from Cell Applications, Inc., and cultured in a fibroblast growth medium (Cell Application, Inc.) at 37°C in 5% CO<sub>2</sub>. HFs stimulation with recombinant BAG3 and with or not H2L4 was performed in Dulbecco's modified Eagle's medium (DMEM) serum-free at indicated concentrations and times. For the collection of conditioned media (CM), HFs ( $4.4 \times 10^5$  cells) were plated in 60-mm tissue culture dishes under standard growth conditions, and after 24 h medium was replaced with DMEM serum-free with BAG3 10 µg/ml (CM-BAG3) or vehicle (CM-PBS) for 48 h. Thereafter, the supernatants were collected, centrifugated at 3000g for 10 min at 4°C, filtered using a 0.2 µm Ministart sterile filter (Sartorius), and stored at -80°C until usage. HF cells were washed with PBS, exposed to trypsin/EDTA (0.05/0.02%) for 0, 3, and 20 min and the detached cells were manually counted by trypan blue staining assay.<sup>9</sup> The human pancreatic cancer cell line MIA PaCa-2 was obtained from the ATCC cell bank and cultured in DMEM supplemented with 10% FBS at 37°C in 5% CO<sub>2</sub>.

## 2.4 | Cytokines determination

The RNA from HFs was isolated using RNeasy® Mini Kit (QIAGEN), followed by complementary DNA (cDNA) synthesis using RT<sup>2</sup> First Strand Kit (QIAGEN). The obtained cDNA was taken for real-time PCR using RT<sup>2</sup> SYBR Green qPCR Mastermix on CFX Real-Time PCR Detection Systems. Primers were supplied by QIAGEN. The protein content of cytokines/chemokines in the supernatant of HFs after BAG3 treatment was determined by ELISA according to the provided instructions. ELISA kits for interleukin-6 (IL-6) and C-C motif chemokine ligand 2 (CCL2) were purchased from Invitrogen and for hepatocyte growth factor (HGF) from RayBiotech.

## 2.5 | Cell viability

Cell proliferation was assessed by [3-(4,5-dimethylthiazol-2-yl)-2,5-diphenyl tetrazolium bromide] (MTT) assay (Sigma-Aldrich). HF cells were seeded in 96-well plates  $5 \times 10^3$  cell/well under standard growth conditions for 24 h at 37°C in 5% CO<sub>2</sub>. Afterward, HF cells were treated in DMEM serum-free with BAG3 at 10 µg/ml or PBS for 24, 48, and 72 h. MIA PaCa-2 cells were seeded in 96-well plates  $5 \times 10^3$  cell/well, for 24 h under standard growth conditions and then incubated with CM of BAG3 or vehicle-treated fibroblasts for 48 h. At the end of the incubation period, cells were incubated with 100 µl of MTT solution (medium serum-free with 0.5 mg/ml of MTT) for further 2 h. After removal of MTT solution, 100 µl of dimethyl sulfoxide was added to the wells for 10 min and the absorbance at 570 nm was measured using a multiplate reader.

## 2.6 | Confocal microscopy

HF cells cultured under standard growth conditions were plated on glass coverslips at 70% of confluence and were allowed to grow for 24 h at 37°C in 5% CO<sub>2</sub>. Cells were treated with BAG3 at 10 µg/ml in DMEM without serum for 48 h. At the end of treatments, cells were fixed with 4% paraformaldehyde in PBS, for 15 min, at RT, washed and permeabilized with 0.25% Triton X-100 in PBS for 5 min at RT. Then, cells were incubated with goat serum 5% in PBS as blocking solution for 60 min at RT and, afterward, were incubated overnight with primary antibodies at 4°C: anti-vimentin (1:100; Cell Signaling Technology, Inc.) and anti-tubulin (1:100; Cell Signaling Technology, Inc.). The secondary antibody was anti-rabbit IgG AlexaFluor-488 conjugated (1:200; Invitrogen, Life Technologies). To visualise the actin cytoskeleton, phalloidin-tetramethylrhodamine B isothiocyanate was used. Coverslips were mounted with Prolong Gold Antifade Reagent as well as diamidino-2-phenylindole (Thermo Fisher Scientific, Inc.) to visualise nuclei. Images were acquired with a Zeiss LSM880 confocal microscope (Zeiss) using 488, 543, and 633-nm lasers. Detector gain voltages and pinhole were set at the beginning of the experiment and maintained constant during the acquisition of all samples.

## 2.7 | Migration assay by transwell

Cell migration assays were measured in Corning transwell permeable support chambers with 8-micron-porefilters (Corning Incorporated Life Sciences). Briefly, cells in serum-free DMEM were seeded into the top chamber ( $1.3 \times 10^5$  cells/well) and DMEM serum-free (negative

control), DMEM with 10% FBS (positive control), CM-BAG3, and CM-vehicle were added to the lower chamber. After incubation for 24 h, the cells on the upper surface were removed using a cotton swab. The migrated cells on the lower surfaces of inserts were fixed with ice-cold methanol and stained with crystal violet. The migrated cells were photographed and counted in 10 representative microscopic fields. The migrated cells were also quantified by colorimetric assay. To this aim, the inserts with fixed and stained cells were filled with 750 µl 10% acetic acid and incubated for 10 min while careful shaking. The eluent from the lower chamber was transferred to a 96-well clear microplate (Corning), and the absorbance at 590 nm was measured using a plate reader.

## 3 | RESULTS

### 3.1 | Expression, purification, and characterisation of recombinant BAG3

To study the role of BAG3 in the cross talk between PDAC and HF cells, we decided to use a recombinant BAG3. To this aim, BAG3 was cloned into a baculovirus expression system by homologous recombination and transfected into sf9 insect cells (see Section 2). BAG3-expressing baculovirus was generated and used to infect sf9 cells and produce large amounts of recombinant protein. Western blotting analysis revealed high amounts of BAG3 both in cell lysate and into the growth medium (Figure 1A) suggesting that a consistent fraction of the protein is secreted. Recombinant BAG3 from pooled cell lysate and CM was affinity purified by means of the polyhistidine tag present at the C-terminus of the protein (Figure 1B). The identity and purity of the recombinant BAG3 were assessed by Coomassie blue staining of SDS-PAGE, Western blot analysis, and LC-MS (Figure 1B,C and Figure S1). These analyses confirmed the authenticity of purified BAG3 (protein sequence coverage by MS/MS of ~60%) and purity of over 90% (Figure S1). From now on we used this BAG3 expressed in baculovirus system in all experiments, except when differently specified.

The functional activity of recombinant BAG3 was examined on human monocytes. Monocytes were treated overnight with different doses of recombinant BAG3 and the release of IL-6 in the growth medium was measured by ELISA. BAG3 induced a dose-dependent release of IL-6 already at 1 µg/ml and reached a plateau at 10 µg/ml (Figure 2A). To validate that IL-6 production was dependent on BAG3 rather than some undefined contaminants, the treatment was repeated in the presence of the BAG3 blocking antibody H2L4.<sup>7</sup> Indeed, H2L4 inhibited the production of IL-6 from BAG3 treated monocytes (Figure 2B).

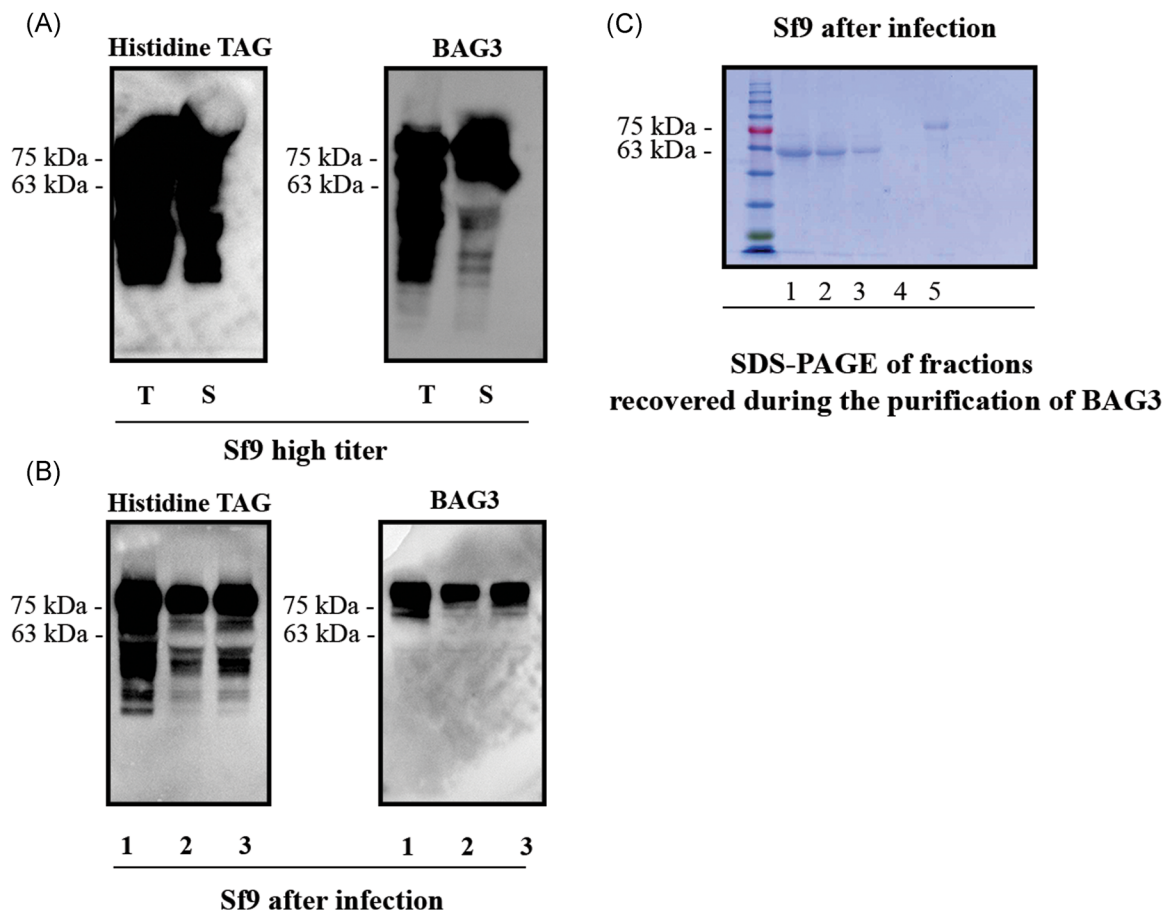


**FIGURE 1** BAG3 expression and purification using the baculovirus-insect cell expression system. (A) Immunoblot using anti-histidine tag and anti-BAG3 antibodies of cellular (T) and secreted BAG3 (S) expressed in Sf9 infected with recombinant BAG3 baculovirus. (B) Immunoblot using anti-histidine tag and anti-BAG3 antibodies of three purification batches (Lanes 1, 2, and 3). (C) SDS-PAGE analysis of recombinant BAG3 produced in Sf9 cells, purified by affinity and stained with Coomassie blue. Protein molecular weight standards, Lane 1: total extract, Lane 2: unbound fraction, Lanes 3–4: wash fractions, and Lane 5: elution fraction are shown. SDS-PAGE, sodium dodecyl sulphate–polyacrylamide gel electrophoresis

As further control monocytes were treated with the same concentration of a recombinant BAG3 produced in *Escherichia coli* (*E. coli*) (coliBAG3) and already used in our previous study.<sup>7</sup> The recombinant BAG3 isolated from baculovirus appears to be more active than BAG3 produced in *E. coli* (Figure 2B) possibly because eukaryotic Sf9 cells are more accurate in folding human proteins and can introduce posttranslational functional modifications.

### 3.2 | BAG3 contributes to the microenvironment of PDAC by inducing the secretion of proinflammatory cytokines and growth factors

We hypothesised that besides monocytes, also the contact of BAG3 with HF might contribute to the typical PDAC tumour microenvironment dominated by

active inflammatory processes. Therefore, HF cells were treated with different concentrations of recombinant BAG3, and the production of IL-6 was quantitated by ELISA, as reported for monocytes. The time-course analysis showed an accumulation of IL-6 in the growth medium of HF cells after 24 h of treatment with BAG3 (Figure 2C), IL-6 was further increased after 48 h of treatment (Figure 2D). The use of the H2L4 antibody was able to prevent the release of IL-6 confirming that we are dealing with a BAG3-mediated response (Figure 2E). These data suggest that BAG3 also exploits HF cells to shape the tumour microenvironment. Previous studies focussed on stroma–tumour interactions reported anticancer effects of HGF and CCL2 inhibition in PDAC<sup>10,11</sup> Therefore, to identify other possible mediators released by the HF cells treated with BAG3, we evaluated the expression of CCL2 and HGF by real-time

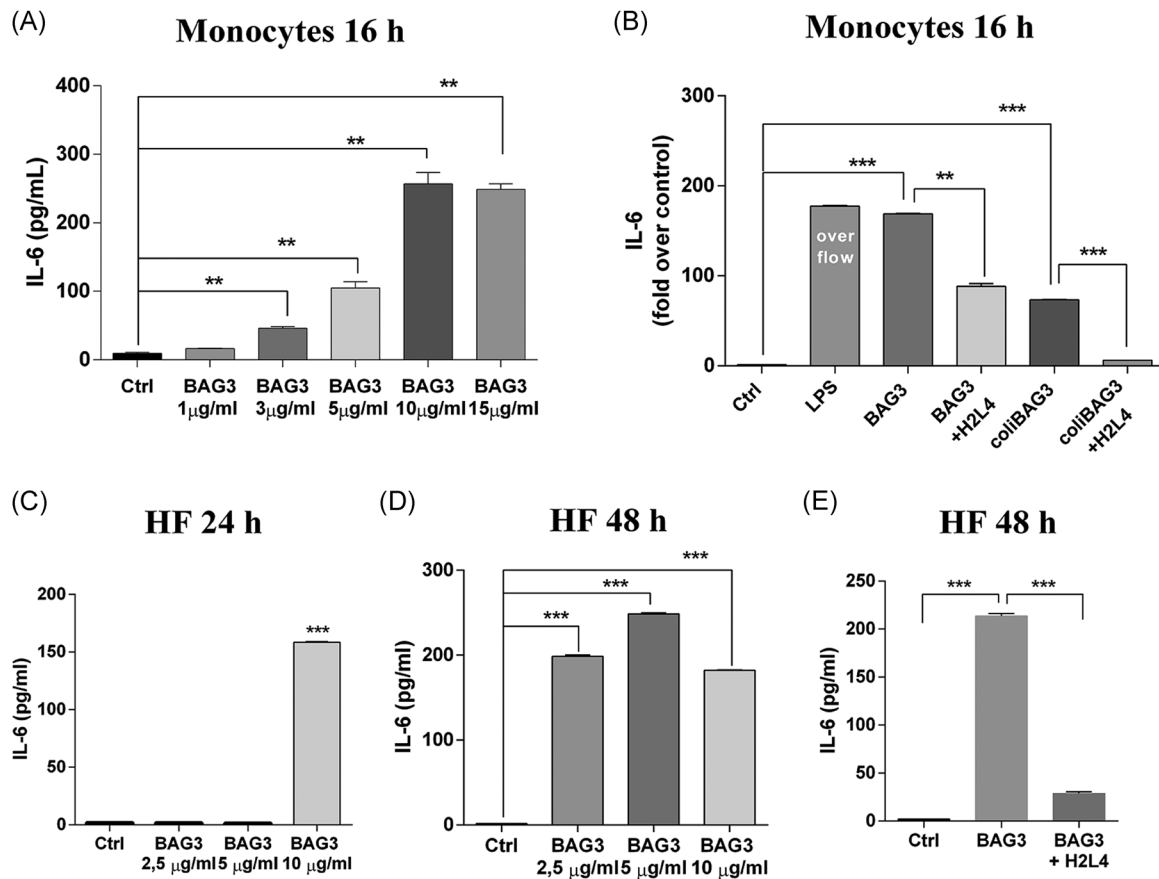
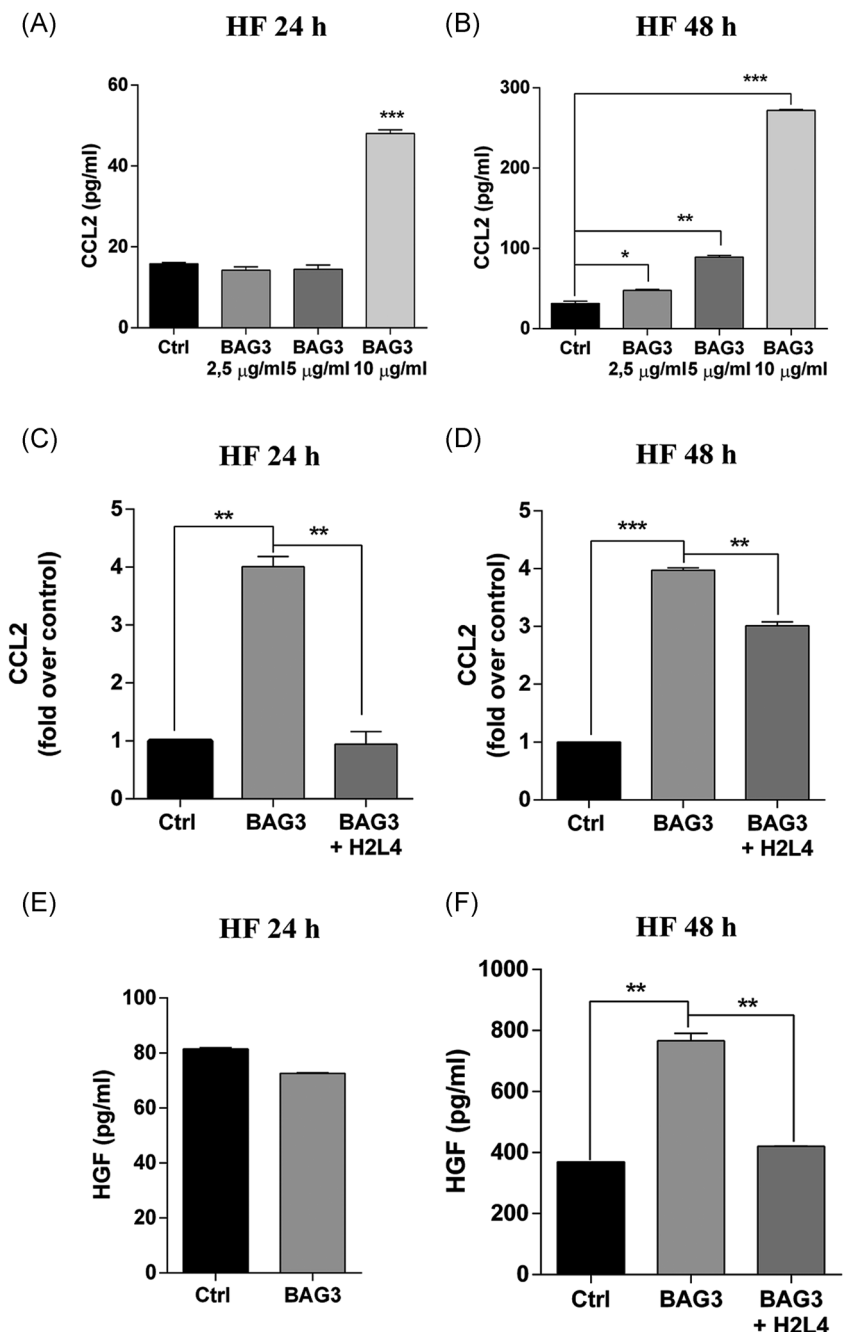


**FIGURE 2** Recombinant BAG3 induces a dose-dependent release of IL-6 in monocytes and in fibroblasts. (A) IL-6 levels released after treatments with increased doses of BAG3 (1, 3, 5, and 10–15 µg/ml for 16 h) were analysed by ELISA. (B) IL-6 levels (fold-over control) released from monocytes stimulated with BAG3 (15 µg/ml) and preincubated or not with H2L4 (320 µg/ml for 30 min). Comparative functional activity between BAG3 produced in baculovirus and recombinant produced in *Escherichia coli* is also shown. IL-6 levels were released by fibroblasts treated with increasing doses of BAG3 (2.5, 5, and 10 µg/ml) for 24 (C) and 48 (D) hours. (E) Experiment like in (D) preincubated or not with H2L4 (320 µg/ml for 30 min). Data reported in this figure are the mean  $\pm$  SE of at least three independent experiments, each performed in triplicate. Ctrl, control; ELISA, enzyme-linked immunosorbent assay; HF, human fibroblast; IL-6, interleukin-6; LPS, lipopolysaccharide. \*\* $p < .01$ , \*\*\* $p < .001$

PCR. Both CCL2 and HGF were upregulated in HF cells treated for 24 h with 10 µg/ml of recombinant BAG3 (Figure S2). The production of CCL2 was validated at the protein levels by ELISA of growth medium of HF cells treated for 24 and 48 h with different doses of BAG3 (Figure 3A,B). After 24 h, CCL2 was detectable only in cells treated with 10 µg/ml of BAG3 (Figure 3A), while after 48 h of treatment, even 2.5 µg/ml was sufficient to significantly increase CCL2 (Figure 3B). The accumulation of CCL2 in the growth medium increased by about six times from 24 to 48 h. Different from IL-6, whose accumulation after 24 or 48 h of stimulation is comparable, the production of CCL2 lasts longer and is more pronounced at

longer time points. Finally, the release/accumulation of CCL2 induced by BAG3 treatment was inhibited when the stimulation was done in the presence of H2L4 antibody (Figure 3C,D). H2L4 completely blocked the accumulation of CCL2 in HF cells stimulated for 24 h, while it was much less effective in cells stimulated for 48 h (Figure 3C,D). Finally, also the induction of HGF protein was confirmed by ELISA. HGF was not increased in the growth medium of HF cells treated with 10 µg/ml of BAG3 for 24 h while it reached about 800 pg/ml after 48 h of stimulation (Figure 3E,F). As shown for IL-6 and CCL2, also the BAG3-induced production of HGF was prevented by the blocking antibody H2L4 (Figure 3F).

**FIGURE 3** BAG3 treatment increases the expression of CCL2 and HGF in fibroblasts. (A, B) ELISA of CCL2 released by HF treated with different doses of BAG3 (2.5, 5, and 10  $\mu\text{g}/\text{ml}$ ) for 24 or 48 h as indicated. (C, D) Effects of H2L4 preincubation (320  $\mu\text{g}/\text{ml}$  for 30 min) on the release of CCL2 (24 and 48 h) in HF treated with BAG3 (10  $\mu\text{g}/\text{ml}$ ). (E, F) ELISA of HGF released by HF treated with BAG3 (10  $\mu\text{g}/\text{ml}$ ) for 24 and 48 h, preincubated or not with H2L4 (320  $\mu\text{g}/\text{ml}$  for 30 min). Data reported in this figure are the mean  $\pm$  SE of at least three independent experiments, each performed in triplicate. CCL2, C–C motif chemokine ligand 2; Ctrl, control; ELISA, enzyme-linked immunosorbent assay; HF, human fibroblast; HGF, hepatocyte growth factor.  $**p < .01$ ,  $***p < .001$



### 3.3 | BAG3 sustains cell survival/proliferation and induces a cytoskeletal reorganisation in fibroblast

Previous studies reported induction of BAG3 expression as a protective mechanism against cellular stress.<sup>12</sup> Along this line, we investigated the effect of BAG3 on the survival/proliferation rate of HF cells cultured in serum-free media. HF cells were treated with 10  $\mu\text{g}/\text{ml}$  of BAG3 and cell number evaluated by MTT assay. After 24 h, the number of HF cells remained the same in both the BAG3-treated and vehicle-treated samples (Figure S3). After 48 and 72 h, the number of cells in vehicle-treated

samples was reduced, while no change was observed in the BAG3-treated sample (Figure S3). These data suggest that BAG3 acts as a prosurvival factor and protects HF cells from death triggered by serum starvation.

We noticed that BAG3-treated fibroblasts underwent gross morphological changes and were more difficult to detach from the plate (Figure S4). We, therefore, investigated the impact of BAG3 on the cytoskeletal organisation of fibroblasts by confocal microscopy (Figure 4A,B). HF cells were plated on glass coverslips and treated with 10  $\mu\text{g}/\text{ml}$  of BAG3 for 48 h and then fixed and stained for vimentin (Figure 4A, Panels b,e), tubulin (Figure 4B, Panels b,e),

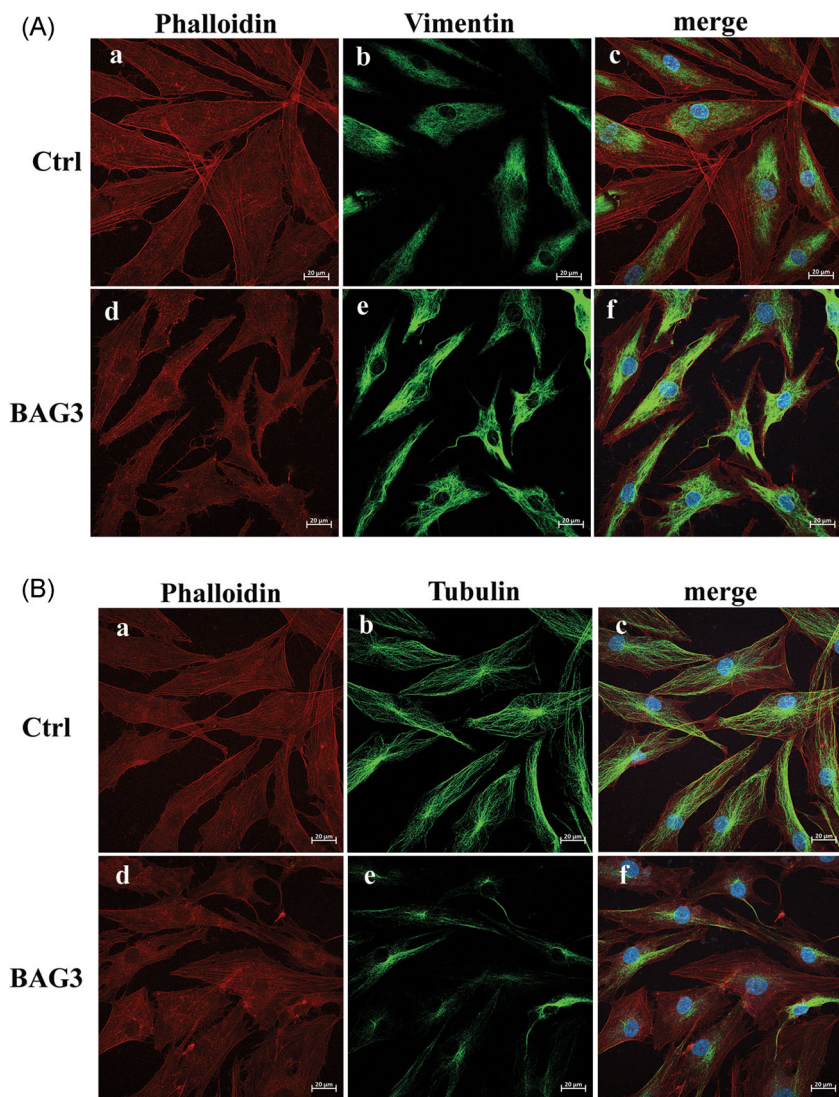


**FIGURE 4** BAG3 induces cytoskeletal reorganisation on fibroblasts. Confocal microscopy images of fibroblasts treated for 48 h with BAG3 (10 μg/ml). (A) Actin was detected by phalloidin–tetramethylrhodamine B isothiocyanate staining (Panels a–d, red), vimentin (b–e) was detected by specific primary antibodies (see Section 2) followed by anti-rabbit IgG AlexaFluor-488 conjugated (green), cells nuclei were stained by DAPI (blue). (B) Actin was detected by phalloidin–tetramethylrhodamine B isothiocyanate staining (Panels a–d, red), tubulin (Panels b–e) was detected by specific primary antibodies (see Section 2) followed by anti-rabbit IgG AlexaFluor-488 conjugated (green), cells nuclei were stained by DAPI (blue). Scale bars = 20 μm. Data reported in this figure are representative of at least three independent experiments. Ctrl, control; DAPI, 4',6-diamidino-2-phenylindole; IgG, immunoglobulin G

and phalloidin (Figure 4A,B, Panels a,d) as markers, respectively, of intermediate filaments, microtubule organisation, and structure of actin microfilaments. BAG3 induced a marked increase of vimentin expression and a detectable expansion of the vimentin network in the cellular peripheral region (Figure 4A, Panels b,c,e,f). Western blot analysis confirmed an increase in vimentin levels and this effect was prevented by the blocking antibody H2L4 (Figure S5). In contrast, microtubules appeared partially depolymerised and mostly concentrated in the perinuclear region (Figure 4B panels b,c,e,f). Actin staining showed an increase of stress-fibres (Figure 4A,B, Panels a,d) according to the reported functional role of BAG3 in the actin folding via interaction with cytosolic chaperonin containing T-complex polypeptide.<sup>13</sup> These data show that BAG3 induces a significant reorganisation of the cytoskeleton accompanied by an increase of adhesion.

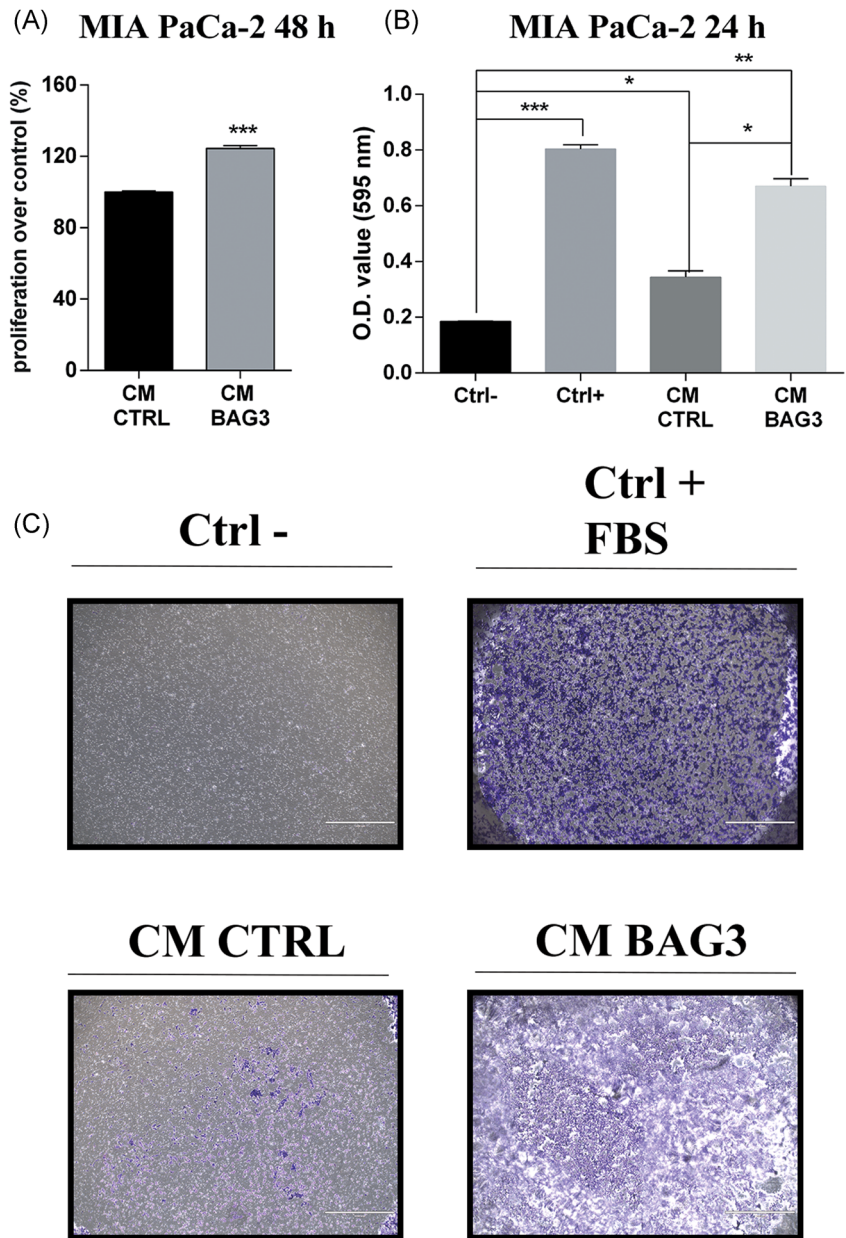
### 3.4 | BAG3-CM stimulate proliferation and cellular migration of PDAC cells

Signals arising from the tumour stromal components can affect tumour biology, stimulating both the proliferation and migration of cancer cells.<sup>5</sup> To determine whether cytokines released by BAG3-treated HF cells act on PDAC cells, HF cells were treated with 10 μg/ml of BAG3 or vehicle for 48 h, CM was collected and used as a growth medium for the MIA PaCa-2 cells (48 h). CM collected from BAG3-treated fibroblasts promoted a significant increase (about 20%) in the proliferation of MIA PaCa-2 (MTT assay) compared to CM collected from vehicle-treated fibroblasts (Figure 5A).

The effect of CM on the motility of MIA PaCa-2 cells was analysed by transwell migration assay. Subconfluent MIA PaCa-2 cells were plated on the top of the transwell membranes and placed on a 24-well plate filled with CM medium.



**FIGURE 5** BAG3-conditioned media stimulates proliferation and cellular migration of MIA PaCa-2 cells. (A) MTT assay showing the proliferation effect of BAG3-conditioned media (48 h) on MIA PaCa-2. (B) Transwell migration assay of MIA PaCa-2 cells exposed for 24 h to BAG3-conditioned media or conditioned media of untreated fibroblasts. (C) Representative images of transwell migration assay described in (B). Data reported in this figure are the mean  $\pm$  SE of at least three independent experiments, each performed in triplicate. Scale bars = 1000  $\mu$ m. CM, conditioned medium; CTRL, control; FBS, fetal bovine serum; OD, optical density. \* $p < .5$ , \*\* $p < .01$ , \*\*\* $p < .001$



After 24 h, cells still present on top of the membranes were removed, while those that migrated through the pores were stained with crystal violet and counted. In addition, the crystal violet was dissolved and quantitated by a spectrophotometer. The CM of BAG3-treated HF showed a strong chemotactic activity and stimulated the migration of MIA PaCa-2 cells in comparison to CM of vehicle-treated HF (Figure 5B,C). Remarkably, the migration of MIA PaCa-2 cells stimulated by CM of BAG3-treated HF was comparable to that stimulated by 10% of serum used as a positive control (Figure 5B,C). We would like to underline that BAG3 treatments were performed in a serum-free medium, thus the cytokines released from BAG3-treated fibroblasts are per se able to sustain the growth and motility of MIA PaCa-2 cells.

It is also worth noting that the CM contains recombinant BAG3 and, therefore, we cannot completely rule out that some of the effects observed on MIA PaCa-2 are directly due to BAG3. However, in our previous study, we reported that PDAC cells normally secrete BAG3, and treatment with recombinant BAG3 does not affect their proliferation. Furthermore, as BAG3 does not function in an autocrine manner, anti-BAG3 monoclonal antibody treatment of PDAC cell lines does not alter their growth.<sup>6</sup> Thus, overall, these data suggest that the effects of the CM are attributable to other factors (IL-6, CCL2, and HGF) known to induce these effects on PDAC cells rather than to a direct BAG3 effect alone.

## 4 | DISCUSSION

Despite significant advances in oncology therapies in recent decades, pancreatic cancer is currently considered an incurable disease with one of the lowest 5-year OS among all cancers. Behind the failure that both clinicians and researchers have experienced for years, there are certainly many factors, including lack of methodology for early diagnosis and lack of effective therapeutics, the latter mostly due to the high tumour heterogeneity and therapy resistance.

Indeed, pancreatic cancer is a remarkably heterogeneous disease and is characterised by significant desmoplasia as well as a highly dense stromal tissue that works as a barrier limiting drug diffusion into target cancer cells.<sup>2</sup> Multiple cell types and signalling molecules are involved in determining this phenotype responsible for cancer aggressiveness and response to therapy. Fibroblasts are certainly one of the cell types involved in shaping the tumour microenvironment,<sup>14</sup> understanding which biological macromolecules and molecular mechanisms are involved in the complex signalling between these cells and the cancer cells are essential to progress towards novel therapeutic approaches.

BAG3 protein is overexpressed in different tumour types and its level has been correlated to tumour resistance to therapy.<sup>15</sup> We have previously shown that BAG3 protein can be secreted by different normal and neoplastic cell types, including PDAC cells<sup>16,17</sup> Furthermore, we have shown in vitro and in vivo that a neutralising BAG3 monoclonal antibody was efficient in delaying tumour growth by reducing the number of tumour infiltrating macrophages,<sup>6,18</sup> thus reducing the pro-survival cytokines produced by these cells. Moreover, in the same in vivo models, we observed a significant reduction of  $\alpha$ -smooth muscle actin expression and collagen deposition in tumour tissue.<sup>19</sup> This observation raised a number of questions on the signalling between fibroblasts and cancer cells: does secreted BAG3 directly affect fibroblast behaviour? What are the signalling pathways activated by fibroblasts in response to BAG3 stimulation? Here, we start answering these questions. Indeed, we show that BAG3 acts directly on fibroblasts inducing changes in their morphology as well as in their survival ability (Figure 6). Moreover, BAG3 induces these cells to secrete cytokines that promote tumour progression, in particular, IL-6, CCL2, and HGF (Figure 6).

It is well known that IL-6 promotes PDAC cells survival and cancer progression<sup>20,21</sup> and high levels of IL-6 and presence of systemic inflammatory response in pancreatic cancer patients have been reported to correlate with worse survival.<sup>22,23</sup> Sources of IL-6 in the tumour microenvironment are both infiltrating

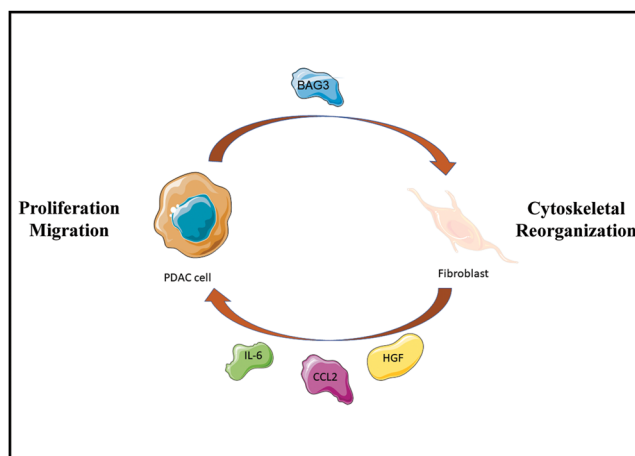


**FIGURE 6** BAG3 induces fibroblasts to secrete interleukin-6 (IL-6), C-C motif chemokine ligand 2 (CCL2), and hepatocyte growth factor (HGF) that promote tumour progression

macrophages<sup>6</sup> and fibroblasts.<sup>19</sup> Now we show that as for macrophages, also for fibroblasts, one of the signalling inducing IL-6 secretion is represented by BAG3 secreted by tumour cells. Of note, the possibility to interfere with pancreatic cancer development using an anti-IL-6 receptor monoclonal antibody, is currently under investigation in a Phase II trial (NCT02767557) in which tocilizumab, is used in combination with a dual first-line gemcitabine/nab-paclitaxel treatment in unresectable locally advanced or metastatic pancreatic cancer patients, it is, therefore, reasonable to imagine that a combination of this drug with the H2L4 anti-BAG3 antibody may improve the outcome.

CCL2 is an important signal for myeloid cell attraction to the tissue microenvironment and recently has been shown that fibroblast activation protein-positive fibroblasts are able to secrete CCL2, thus promoting an immunosuppressive environment.<sup>24</sup> CCL2 is overexpressed in various cancer types, its expression is directly correlated with a worse prognosis, and recently, in several murine tumour models, it has been shown that administration of a CCL2 receptor antagonist (CCR2 small molecule inhibitor RS504393) is able to sensitise and enhance tumour response over anti-PD-1 monotherapy.<sup>25</sup> In line with these findings, we have previously shown that the anti-BAG3 monoclonal antibody, in combination with an anti-PD-1 antibody, results in a potentiated therapeutic effect in a syngeneic pancreatic murine model.<sup>18</sup> Furthermore, CCR2 specific antagonist CCX872 was used in combination with FOLFIRINOX to treat pancreatic nonresectable cancer patients in a clinical Phase Ib multicentre study (NCT02345408) and resulted in an improvement of OS in respect to FOLFIRINOX regimen alone.<sup>26</sup> Again, here we have

shown that CCL2 secretion by fibroblasts is dependent on BAG3, thus suggesting that blocking BAG3 signalling will also interfere with this signalling pathway contributing to the anticancer effect.

Finally, HGF secretion by fibroblasts in pancreatic cancer has been recently shown to promote liver metastases.<sup>27</sup> Moreover and remarkably, has been reported that targeting the HGF/mesenchymal–epithelial transition factor pathway with a blocking antibody a receptor inhibitor in combination with a chemotherapeutic agent, such as gemcitabine, completely eliminated metastasis, and significantly decreased tumour growth in an orthotopic murine model of advanced pancreatic cancer.<sup>28</sup>

In conclusion, our work makes a step forward in the comprehension of the complex picture of tumour–stroma interaction in pancreatic cancer showing that BAG3 acts directly on fibroblasts promoting morphological changes that contribute to the shaping of the tumour stroma. Moreover, BAG3 induces fibroblasts to release IL-6, CCL2, and HGF that concur to promote tumour progression (Figure 6), thus suggesting future potentials use in combination therapy.

#### ACKNOWLEDGMENTS

This study was supported by Associazione Italiana per la Ricerca sul Cancro (AIRC IG-20043; to Vincenzo De Laurenzi). This study was supported in part by POR CAMPANIA FESR 2014–2020 “SYSTEM INNOVATION FOR CANCER EARLY DIAGNOSIS SICED” to Liberato Marzullo, Alessandra Rosati, and Maria C. Turco. Open access funding provided by Università degli Studi Gabriele d'Annunzio Chieti Pescara within the CRUI-CARE Agreement.

#### CONFLICT OF INTERESTS

Margot De Marco, Liberato Marzullo, Alessandra Rosati, and Maria C. Turco are shareholders of BIOUNIVERSA s.r.l. that provided the anti-BAG3 humanised mAb. Other authors declare that there are no conflict of interests.

#### AUTHOR CONTRIBUTIONS

*Performed the experiments, interpreted data, and wrote the paper:* Beatrice Dufrosine. *Performed the experiments:* Verena Damiani. *Performed the confocal imaging:* Emily Capone. *Performed the mass spectrometry analyses:* Damiana Pieragostino. *Edited the manuscript:* Margot De Marco, Francesca Reppucci, Maria C. Turco, Alessandra Rosati, Liberato Marzullo, and Enrico Dainese. *Suggested ideas and wrote the paper:* Gianluca Sala. *Supervised the study and wrote the manuscript:* Michele Sallese. *Designed and supervised the study and edited the manuscript:* Vincenzo De Laurenzi. All authors have read and agreed to the published version of the manuscript.

#### DATA AVAILABILITY STATEMENT

The data that support the findings of this study are available from the corresponding author upon reasonable request.

#### ORCID

Maria C. Turco  <http://orcid.org/0000-0002-7835-359X>

Alessandra Rosati  <http://orcid.org/0000-0001-6675-0857>

Michele Sallese  <http://orcid.org/0000-0002-2555-3571>

#### REFERENCES

- Sung H, Ferlay J, Siegel RL, et al. Global cancer statistics 2020: GLOBOCAN estimates of incidence and mortality worldwide for 36 cancers in 185 countries. *CA Cancer J Clin.* 2021;1-41. doi:10.3322/caac.21660
- Bulle A, Lim KH. Beyond just a tight fortress: contribution of stroma to epithelial-mesenchymal transition in pancreatic cancer. *Signal Transduct Target Ther.* 2020;5(1):249. doi:10.1038/s41392-020-00341-1
- Cid-Arregui A, Juarez V. Perspectives in the treatment of pancreatic adenocarcinoma. *World J Gastroenterol.* 2015; 21(31):9297-9316. doi:10.3748/wjg.v21.i31.9297
- Liang C, Shi S, Meng Q, et al. Complex roles of the stroma in the intrinsic resistance to gemcitabine in pancreatic cancer: where we are and where we are going. *Experimental and Molecular Medicine.* 2017;49(12):406. doi:10.1038/emm.2017.255
- Chu GC, Kimmelman AC, Hezel AF, DePinho RA. Stromal biology of pancreatic cancer. *J Cell Biochem.* 2007;101(4): 887-907. doi:10.1002/jcb.21209
- Rosati A, Basile A, D'auria R, et al. BAG3 promotes pancreatic ductal adenocarcinoma growth by activating stromal macrophages. *Nat Commun.* 2015;6:1-11. doi:10.1038/ncomms9695
- Basile A, De Marco M, Festa M, et al. Development of an anti-BAG3 humanized antibody for treatment of pancreatic cancer. *Mol Oncol.* 2019;13(6):1388-1399. doi:10.1002/1878-0261.12492
- Pieragostino D, Lanuti P, Cicalini I, et al. Proteomics characterization of extracellular vesicles sorted by flow cytometry reveals a disease-specific molecular cross-talk from cerebrospinal fluid and tears in multiple sclerosis. *J Proteomics.* 2019;204:103403. doi:10.1016/j.jprot.2019.103403
- Löffek S, Hurskainen T, Jackow J, et al. Transmembrane collagen XVII modulates integrin dependent keratinocyte migration via PI3K/Rac1 signaling. *PLoS One.* 2014;9(2):1-11. doi:10.1371/journal.pone.0087263
- Pothula SP, Xu Z, Goldstein D, et al. Hepatocyte growth factor inhibition: a novel therapeutic approach in pancreatic cancer. *Br J Cancer.* 2016;114(3):269-280. doi:10.1038/bjc.2015.478
- Pausch TM, Aue E, Wirsik NM, et al. Metastasis-associated fibroblasts promote angiogenesis in metastasized pancreatic cancer via the CXCL8 and the CCL2 axes. *Sci Rep.* 2020;10(1): 1-12. doi:10.1038/s41598-020-62416-x
- Ammirante M, Rosati A, Arra C, et al. IKK $\gamma$  protein is a target of BAG3 regulatory activity in human tumor growth. *Proc Natl Acad Sci USA.* 2010;107(16):7497-7502. doi:10.1073/pnas.0907696107

13. Fontanella B, Birolo L, Infusini G, et al. The co-chaperone BAG3 interacts with the cytosolic chaperonin CCT: new hints for actin folding. *Int J Biochem Cell Biol.* 2010;42(5):641-650. doi:10.1016/j.biocel.2009.12.008
14. Biffi G, Tuveson DA. Diversity and biology of cancer-associated fibroblasts. *Physiol Rev.* 2021;101(1):147-176. doi:10.1152/physrev.00048.2019
15. De Marco M, Turco MC, Marzullo L. BAG3 in tumor resistance to therapy. *Trends Cancer.* 2020;6(12):985-988. doi:10.1016/j.trecan.2020.07.001
16. Falco A, Rosati A, Festa M, et al. BAG3 is a novel serum biomarker for pancreatic adenocarcinomas. *Am J Gastroenterol.* 2013;108(7):1178-1180. doi:10.1038/ajg.2013.128
17. De Marco M, Falco A, Basile A, et al. Detection of soluble BAG3 and anti-BAG3 antibodies in patients with chronic heart failure. *Cell Death Dis.* 2013;4(2):e495. doi:10.1038/cddis.2013.8
18. Iorio V, Rosati A, D'Auria R, et al. Combined effect of anti-BAG3 and anti-PD-1 treatment on macrophage infiltrate, CD8+ T cell number and tumour growth in pancreatic cancer. *Gut.* 2018;67(4):780-782. doi:10.1136/gutjnl-2017-314225
19. Iorio V, De Marco M, Basile A, et al. CAF-derived IL6 and GM-CSF cooperate to induce M2-like TAMs-letter. *Clin Cancer Res.* 2019;25(2):892-893. doi:10.1158/1078-0432.CCR-18-2455
20. Zhang Y, Yan W, Collins MA, et al. Interleukin-6 is required for pancreatic cancer progression by promoting MAPK signaling activation and oxidative stress resistance. *Cancer Res.* 2013;73(20):6359-6374. doi:10.1158/0008-5472.CAN-13-1558-T
21. van Duijneveldt G, Griffin MDW, Putoczki TL. Emerging roles for the IL-6 family of cytokines in pancreatic cancer. *Clin Sci.* 2020;134(16):2091-2115. doi:10.1042/CS20191211
22. Ebrahimi B, Tucker SL, Li D, Abbruzzese JL, Kurzrock R. Cytokines in pancreatic carcinoma: correlation with phenotypic characteristics and prognosis. *Cancer.* 2004;101(12):2727-2736. doi:10.1002/cncr.20672
23. Talar-Wojnarowska R, Gasiorowska A, Smolarz B, Romanowicz-Makowska H, Kulig A, Malecka-Panas E. Clinical significance of interleukin-6 (IL-6) gene polymorphism and IL-6 serum level in pancreatic adenocarcinoma and chronic pancreatitis. *Dig Dis Sci.* 2009;54(3):683-689. doi:10.1007/s10620-008-0390-z
24. Yang X, Lin Y, Shi Y, et al. FAP Promotes immunosuppression by cancer-associated fibroblasts in the tumor microenvironment via STAT3-CCL2 signaling. *Cancer Res.* 2016;76(14):4124-4135. doi:10.1158/0008-5472.CAN-15-2973
25. Tu MM, Abdel-Hafiz HA, Jones RT, et al. Inhibition of the CCL2 receptor, CCR2, enhances tumor response to immune checkpoint therapy. *Communications Biology.* 2020;3(1):1-12. doi:10.1038/s42003-020-01441-y
26. Linehan D, Smith NM, Hezel AF, et al. Overall survival in a trial of orally administered CCR2 inhibitor CCX872 in locally advanced/metastatic pancreatic cancer: correlation with blood monocyte counts. *J Clin Oncol.* 2018;36(5):92. doi:10.1200/JCO.2018.36.5\_suppl.92
27. Bhattacharjee S, Mederacke I, Schwabe RF. Tumor restriction by type I collagen opposes tumor-promoting effects of cancer-associated fibroblasts. *J Clin Invest.* 2021;131. doi:10.1172/JCI146987
28. Xu Z, Pang TCY, Liu AC, et al. Targeting the HGF/c-MET pathway in advanced pancreatic cancer: a key element of treatment that limits primary tumour growth and eliminates metastasis. *Br J Cancer.* 2020;122(10):1486-1495. doi:10.1038/s41416-020-0782-1

## SUPPORTING INFORMATION

Additional supporting information may be found in the online version of the article at the publisher's website.

**How to cite this article:** Dufrusine B, Damiani V, Capone E, et al. BAG3 induces fibroblasts to release key cytokines involved in pancreatic cell migration. *J Cell Biochem.* 2022;123:65-76. doi:10.1002/jcb.30172